Cell Reports, Volume *31*

Supplemental Information

Distinct Roles for *Rac1* in Sertoli Cell Function during Testicular Development and Spermatogenesis

Anna Heinrich, Sarah J. Potter, Li Guo, Nancy Ratner, and Tony DeFalco

Figure S1

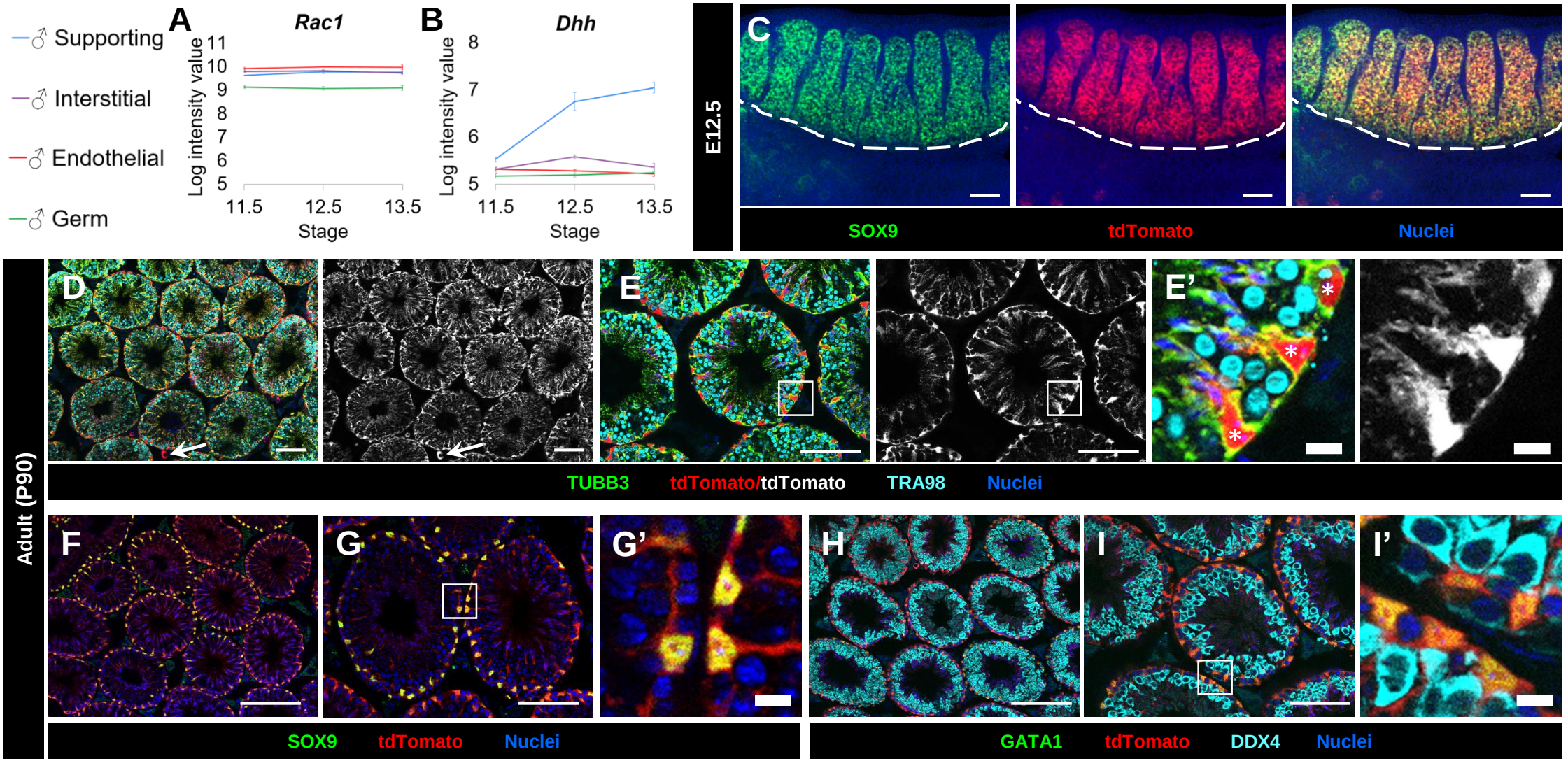
♂ Supporting
♂ Interstitial
♂ Endothelial
♂ Germ
A
Rac1
Log intensity value
11
10
9
8
7
6
5
11.5
12.5
13.5
Stage
B
Dhh
Log intensity value
8
7
6
5
11.5
12.5
13.5
Stage
E12.5
C
SOX9
tdTomato
Nuclei
Adult (P90)
D
E
E'
TUBB3
tdTomato/tdTomato
TRA98
Nuclei
F
G
G'
SOX9
tdTomato
Nuclei
H
I
I'
GATA1
tdTomato
DDX4
Nuclei

Figure S1. *Dhh*-Cre is highly efficient and specific for targeting Sertoli cells, Related to Figure 1.

(A,B) Plots showing gene expression levels of *Rac1* and *Dhh* expression, which were generated from fetal gonad cell-type-specific microarray data (Jameson et al., 2012), where cell lineages (supporting Sertoli cells, interstitial cells, endothelial cells, and germ cells) were independently plotted in different colors. Graph contains data for E11.5, E12.5, and E13.5 XY gonads for each cell type. In general, expression values below 6 are considered background expression levels. *Rac1* is expressed at high levels in all cell types, while *Dhh* becomes highly specific to Sertoli cells early in testicular development. (C-I) Immunofluorescence images of E12.5 (C) and adult P90 (D-I) *Dhh*-Cre; *Rosa*-tdTomato testes. E', G' and I' are higher-magnification images of the boxed regions in E, G, and I. Dashed line in C indicates gonad-mesonephros border. (C) tdTomato specifically co-localizes with Sertoli marker SOX9 in E12.5 fetal testes. (D-I) Lineage tracing of *Dhh*-Cre activity into adulthood reveals highly efficient tdTomato labeling in TUBB3/SOX9/GATA1-positive Sertoli cells, with no labeling in TRA98/DDX4-positive germ cells. We occasionally observed mosaic Cre activity in vasculature-associated cells (arrow in D), as has been previously reported in the testis (Lindeboom et al., 2003). Thin scale bar, 100 μm; thick scale bar 10 μm.

Figure S2

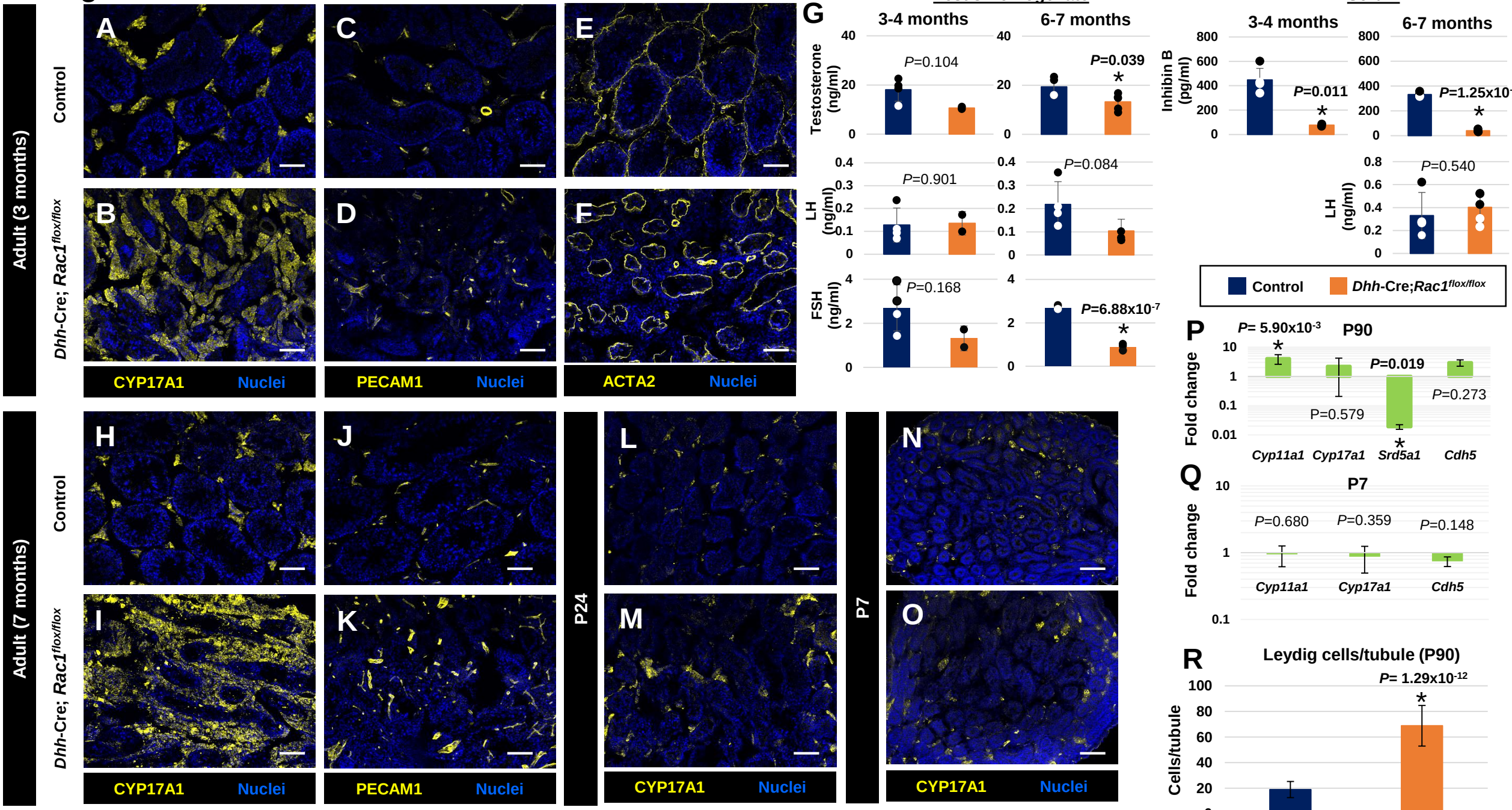
Adult (3 months)
Control
Dhh-Cre; Rac1flox/flox
A
B
C
D
E
F
CYP17A1
Nuclei
PECAM1
Nuclei
ACTA2
Nuclei
G
Testis Homogenate
3-4 months
6-7 months
Testosterone (ng/ml)
P=0.104
P=0.039
LH (ng/ml)
P=0.901
P=0.084
FSH (ng/ml)
P=0.168
P=6.88x10-7
Serum
3-4 months
6-7 months
Inhibin B (pg/ml)
P=0.011
P=1.25x10-8
LH (ng/ml)
P=0.540
Control
Dhh-Cre;Rac1flox/flox
Adult (7 months)
Control
Dhh-Cre; Rac1flox/flox
H
I
J
K
CYP17A1
Nuclei
PECAM1
Nuclei
P24
L
M
CYP17A1
Nuclei
P7
N
O
CYP17A1
Nuclei
P
P90
P= 5.90x10-3
P=0.579
P=0.019
P=0.273
Fold change
Cyp11a1
Cyp17a1
Srd5a1
Cdh5
Q
P7
P=0.680
P=0.359
P=0.148
Fold change
Cyp11a1
Cyp17a1
Cdh5
R
Leydig cells/tubule (P90)
P= 1.29x10-12
Cells/tubule

Figure S2. *Rac1* deletion in Sertoli cells has minimal effects on vascular and Leydig cell development, but disrupts some aspects of hormone production, Related to Figure 1.

(A-F) Immunofluorescence images of 3-month-old (P90) adult control *Dhh*-Cre;*Rac1*$^{flox/+}$ (A,C,E) and *Dhh*-Cre;*Rac1*$^{flox/flox}$ cKO (B,D,F) testes, showing normal expression of CYP17A1 (Leydig cells), PECAM1 (endothelial cells), and ACTA2 (also known as SMA; marker for peritubular myoid cells and vascular smooth muscle). (G) Graphs showing levels of various hormones in testis homogenate or blood serum from control versus cKO adult males. Each dot in the graphs represents an independent testis or serum sample. Left side shows testicular testosterone (T), luteinizing hormone (LH), and follicle-stimulating hormone (FSH) in 3-4 month old (n=2-4) or 6-7 month old (n=2-4) males, with significantly decreased levels of T and FSH only occurring at 6-7 months old. Right side shows significantly decreased levels of serum Inhibin B in both 3-4 month old (n=2-4) and 6-7 month old (n=2-4) males, but normal levels of serum LH in 6-7 month old (n=2-4) males. Data are shown as mean ± SD. *P* values were calculated using a two-tailed Student t-test. (H-K) Immunofluorescence images of 7-month-old adult control *Dhh*-Cre;*Rac1*$^{flox/+}$ (H,J) and *Dhh*-Cre;*Rac1*$^{flox/flox}$ cKO (I,K) testes, showing expression of CYP17A1 and PECAM1. (L,M) Immunofluorescence images of P24 juvenile control *Dhh*-Cre;*Rac1*$^{flox/+}$ (L) and *Dhh*-Cre;*Rac1*$^{flox/flox}$ cKO (M) testes, showing expression of CYP17A1. (N,O) Immunofluorescence images of P7 postnatal control *Rac1*$^{flox/flox}$ (N) and *Dhh*-Cre;*Rac1*$^{flox/flox}$ cKO (O) testes, showing expression of CYP17A1. (P,Q) Quantitative PCR analyses showing fold change of gene expression in controls versus cKO testes (see above for description of controls at each age) at P90 (P) and P7 (Q) for Leydig cell genes *Cyp11a1* (n=5 for P7; n=4 for P90), *Cyp17a1* (n=5 for P7; n=5 for P90), and *Srd5a1* (n=3 for P90) and vascular endothelial *Cdh5* (n=5 for P7; n=3 for P90). (R) Graph showing average number of CYP17A1+ Leydig cells per tubule in control versus cKO P90 testes (n=31, 37, and 30 tubules each from 3 independent control males and n=45, 101, and 65 tubules each from 3 independent cKO males). Data are shown as mean ± SD. *P* values were calculated using a two-tailed Student t-test. Scale bar is 100 μm throughout all panels.

Figure S3

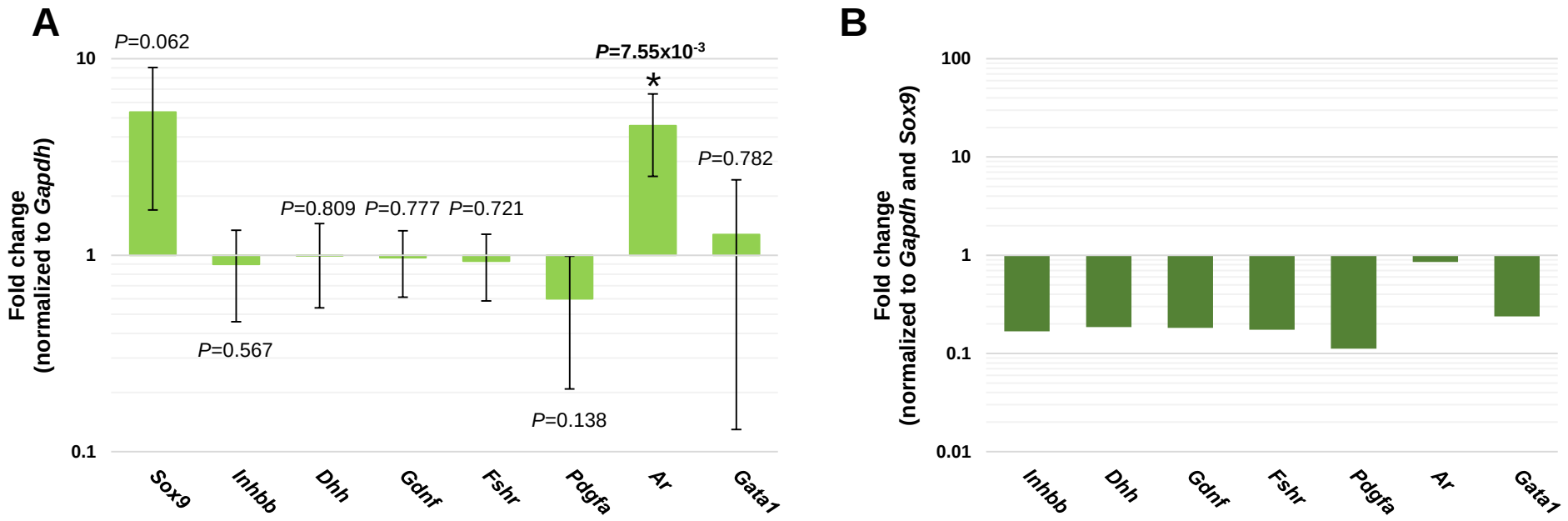
A
P=0.062
P=7.55x10-3
*
P=0.782
P=0.809
P=0.777
P=0.721
P=0.567
P=0.138
10
1
0.1
Fold change
(normalized to Gapdh)
Sox9
Inhbb
Dhh
Gdnf
Fshr
Pdgfa
Ar
Gata1
B
100
10
1
0.1
0.01
Fold change
(normalized to Gapdh and Sox9)
Inhbb
Dhh
Gdnf
Fshr
Pdgfa
Ar
Gata1

Figure S3. Expression of Sertoli-expressed differentiation markers and paracrine factors is reduced in adult cKO testes, Related to Figure 1.

(A) qPCR analyses of P90 *Dhh*-Cre;*Rac1*$^{flox/+}$ control versus *Dhh*-Cre;*Rac1*$^{flox/flox}$ cKO testes, focusing on genes expressed in Sertoli cells, encoding transcription factors (*Sox9*, *Gata1*), hormone receptors (*Fshr*, *Ar*), and paracrine secreted factors (*Inhbb*, *Dhh*, *Gdnf*, *Pdgfa*) (n=6 for *Sox9*; n=3 for *Inhbb*; n=3 for *Dhh*; n=3 for *Gdnf*; n=3 for *Fshr;* n=3 for *Pdgfa*; n=4 for *Ar*; n=3 for *Gata1*). (B) Same data as in A, except data was additionally normalized to *Sox9* (after normalization to *Gapdh*) by average fold change of cKO *Sox9* expression relative to controls. Data are shown as mean ± SD in A, and as mean in B. *P* values were calculated using a two-tailed Student t-test.

Figure S4

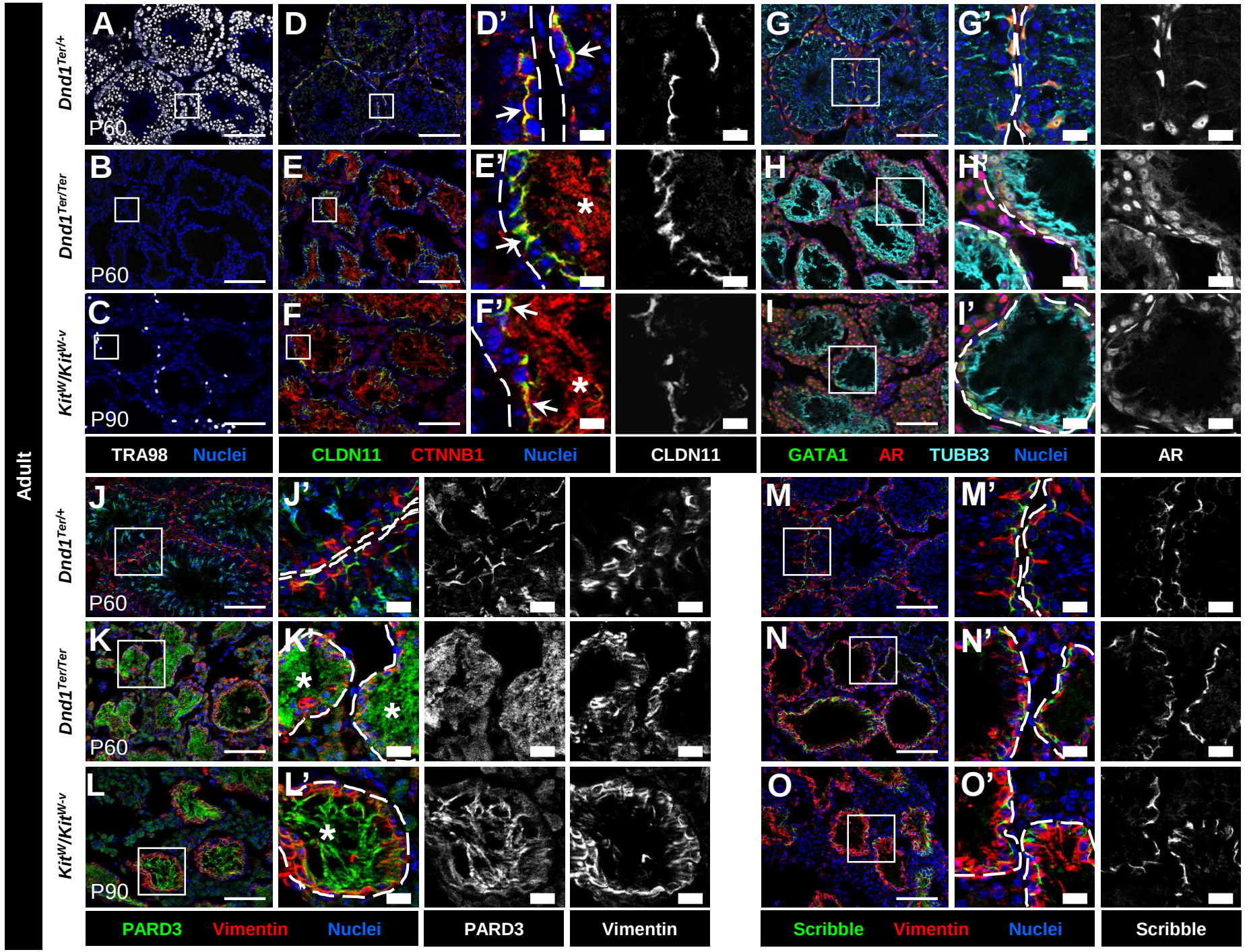
Adult
Dnd1Ter/+
Dnd1Ter/Ter
KitW/KitW-v
P60
P90
A
B
C
D
D'
E
E'
F
F'
G
G'
H
H'
I
I'
J
J'
K
K'
L
L'
M
M'
N
N'
O
O'
TRA98 Nuclei
CLDN11 CTNNB1 Nuclei
CLDN11
GATA1 AR TUBB3 Nuclei
AR
PARD3 Vimentin Nuclei
PARD3
Vimentin
Scribble Vimentin Nuclei
Scribble

Figure S4. Localization of apicobasal polarity markers and BTB proteins are mostly, but not completely, maintained in mouse models of germ cell deficiency, Related to Figure 4.

(A-O) Immunofluorescent images of P60 *Dnd1*$^{Ter/+}$ control (A,D,G,J,M), P60 *Dnd1*$^{Ter/Ter}$ mutant (B,E,H,K,N), and P90 *Kit*^{W}/*Kit*$^{W\text{-}v}$ compound heterozygous mutant (C,F,I,L,O) testes. D'-O' are higher-magnification images of the boxed regions in D-O. Dashed lines throughout indicate tubule boundaries. (A-C) TRA98 staining reveals extent of germ cell loss in *Ter* and *Kit* mutants. (D-F) CLDN11/CTNNB1 staining outlines normal BTB structure in all models (arrows); however, CTNNB1 expression is also expanded throughout Sertoli cells in germ-cell-deficient testes (asterisks in E' and F'). (G-I) AR nuclear localization is largely maintained in Sertoli cells in all models, although some weak cytoplasmic expression is observed in germ-cell-deficient testes. (J-L) While basal localization of Vimentin is maintained in all samples, PARD3 localization is perturbed in germ-cell-deficient testes (asterisks in K' and L'). (M-O) Scribble expression is maintained normally, i.e., along the BTB and in the basal compartment, in all testes. Thin scale bar, 100 μm; thick scale bar 10 μm.

Figure S5

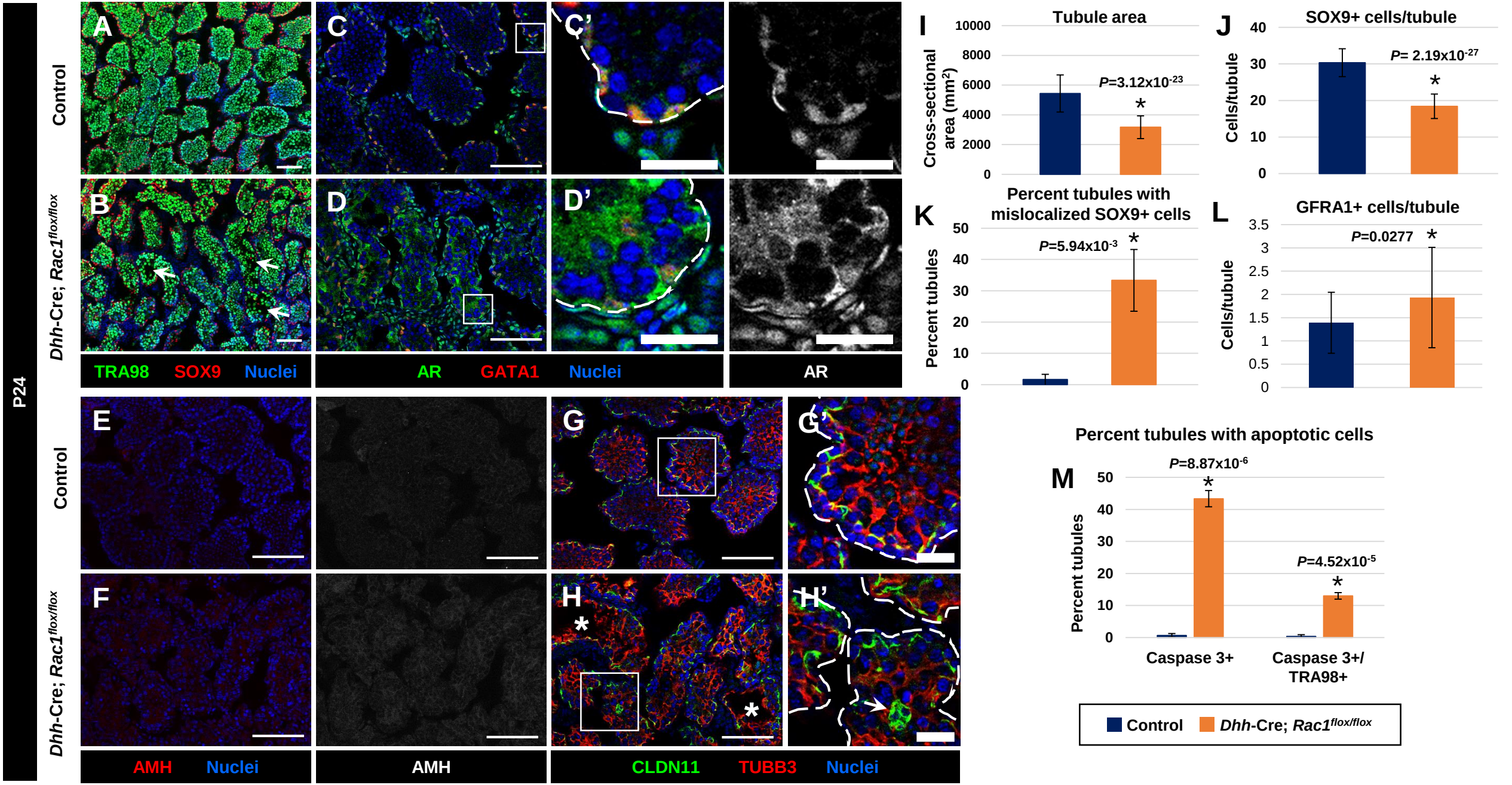
P24
Control
Dhh-Cre; Rac1flox/flox
A
B
C
C'
D
D'
TRA98 SOX9 Nuclei
AR GATA1 Nuclei
AR
E
F
G
G'
H
H'
AMH Nuclei
AMH
CLDN11 TUBB3 Nuclei
I
Tubule area
Cross-sectional area (mm2)
10000
8000
6000
4000
2000
0
P=3.12x10-23
J
SOX9+ cells/tubule
Cells/tubule
40
30
20
10
0
P= 2.19x10-27
K
Percent tubules with mislocalized SOX9+ cells
Percent tubules
50
40
30
20
10
0
P=5.94x10-3
L
GFRA1+ cells/tubule
Cells/tubule
3.5
3
2.5
2
1.5
1
0.5
0
P=0.0277
M
Percent tubules with apoptotic cells
Percent tubules
50
40
30
20
10
0
P=8.87x10-6
P=4.52x10-5
Caspase 3+
Caspase 3+/ TRA98+
Control
Dhh-Cre; Rac1flox/flox

Figure S5. Onset of testis dysgenesis is evident in juvenile (P24) *Rac1* cKO males, Related to Figure 6.

(A-H) Immunofluorescence images of P24 control *Dhh*-Cre;*Rac1*$^{flox/+}$ (A,C,E,G) and *Dhh*-Cre;*Rac1*$^{flox/flox}$ cKO (B,D,F,H) testes. C', D', G', and H' are higher-magnification images of the boxed regions in C, D, G, and H. Dashed lines throughout indicate tubule boundaries. (A,B) TRA98 staining reveals patchy germ cell loss in cKO tubules (arrows in B). (C,D) AR subcellular (nuclear) localization is disrupted in cKO tubules. (E,F) AMH expression is not substantially affected in cKO testes. (G,H) CLDN11 staining shows a grossly normal initial formation of the BTB; however, there are aberrant CLDN11 aggregates often seen in the middle of cKO tubules (arrow in H'). Vacuolization of Sertoli cells (TUBB3+) is often seen in cKO tubules (asterisks in H), likely due to germ cell loss. Thin scale bar, 100 μm; thick scale bar 25 μm. (I) Graph showing average tubule cross-sectional area of P24 control versus cKO testes (n=20 tubules each from 3 independent males). (J) Graph showing cell counts of SOX9+ cells per tubule in P24 control versus cKO testes (n=15 tubules each from 3 independent males). (K) Graph showing percent of tubules displaying SOX9+ Sertoli cells mislocalizing to the tubule lumen in P24 control versus cKO testes (n=20 tubules each from 3 independent control males and n=50 tubules each from 3 independent cKO males). (L) Graph showing average number of GFRA1+ germ cells per tubule (in tubules that contained GFRA1+ cells) in P24 control versus cKO testes (n=25 tubules each from 3 independent males). (M) Graph showing percent tubules containing cleaved Caspase 3+ cells and cleaved Caspase 3+/TRA98+ double-positive germ cells in P24 control versus cKO testes (n=50 tubules each from 3 independent males). Data are shown as mean ± SD. *P* values were calculated using a two-tailed Student t-test.

Figure S6

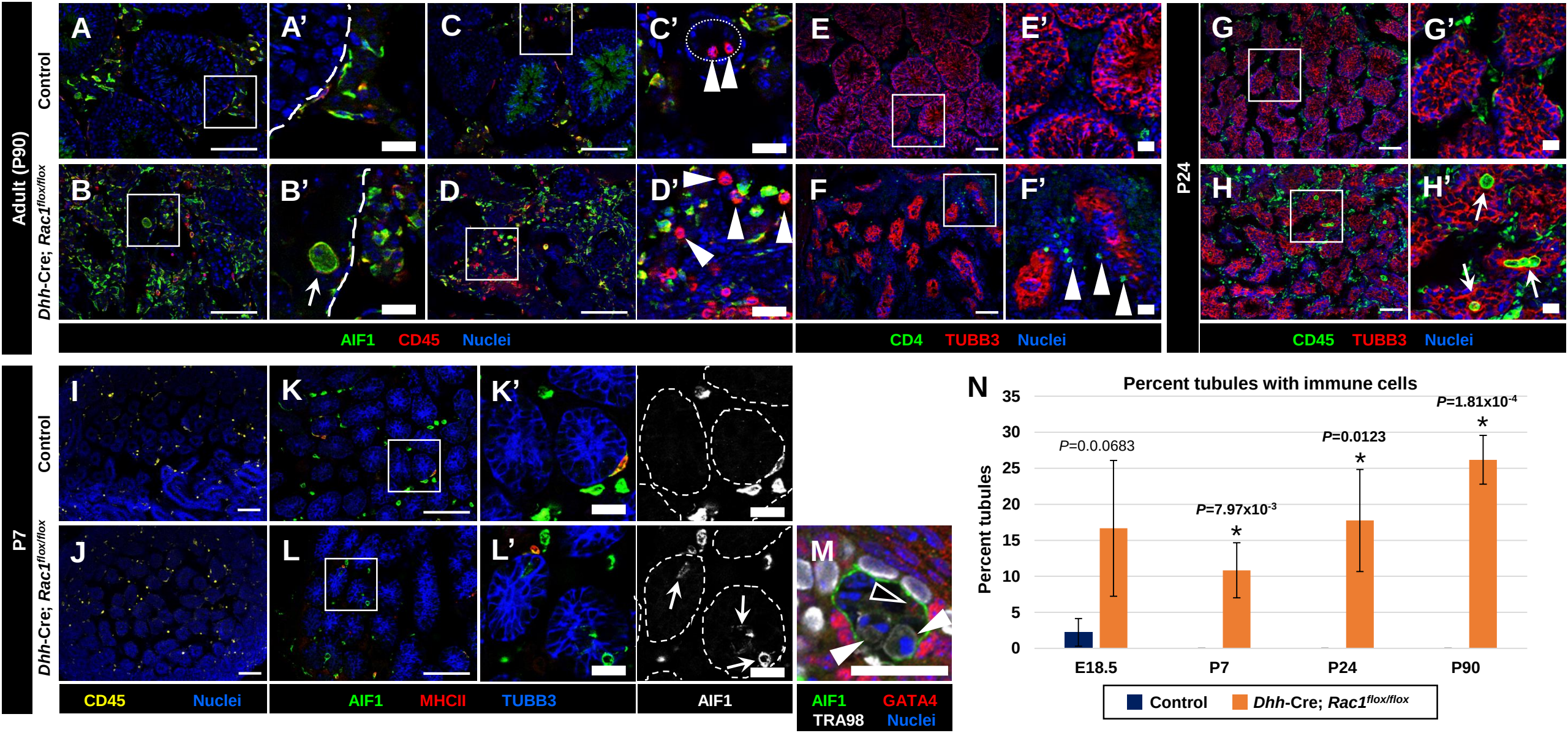
Adult (P90)
Control
Dhh-Cre; Rac1flox/flox
A
A'
C
C'
E
E'
B
B'
D
D'
F
F'
AIF1 CD45 Nuclei
CD4 TUBB3 Nuclei
P24
G
G'
H
H'
CD45 TUBB3 Nuclei
P7
Control
Dhh-Cre; Rac1flox/flox
I
K
K'
J
L
L'
M
CD45 Nuclei
AIF1 MHCII TUBB3
AIF1
AIF1 GATA4
TRA98 Nuclei
N
Percent tubules with immune cells
Percent tubules
35
30
25
20
15
10
5
0
P=0.0.0683
P=7.97x10-3
P=0.0123
P=1.81x10-4
*
E18.5
P7
P24
P90
Control
Dhh-Cre; Rac1flox/flox

Figure S6. Immune cells infiltrate into tubules of *Rac1* cKO testes, Related to Figure 6.

(A-M) Immunofluorescence images of P90 control *Dhh*-Cre;*Rac1*$^{flox/+}$ (A,C,E), P90 *Dhh*-Cre;*Rac1*$^{flox/flox}$ cKO (B,D,F), P24 control *Dhh*-Cre;*Rac1*$^{flox/+}$ (G), P24 *Dhh*-Cre;*Rac1*$^{flox/flox}$ cKO (H), P7 control *Rac1*$^{flox/flox}$ (I,K), and P7 *Dhh*-Cre;*Rac1*$^{flox/flox}$ cKO (J,L,M) testes. A'-H' and K'-L' are higher-magnification images of the boxed regions in A-H and K-L. (A-D) There is an increase in CD45+/AIF1+ macrophages in the adult cKO testis, in particular within the tubule lumen (arrow in B'), which are not observed in controls. (C,D) Round CD45-bright cells are more often seen in the interstitium of adult cKO testes (arrowheads in C' and D'), whereas they are only seen within arterioles in control testes (dashed outline in C'). (E,F) CD4 staining reveals an increase in T cell infiltration in cKO testes (arrowheads in F'). (G,H) P24 cKO testes contain an increased number of CD45+ cells, especially within tubule lumens (arrows in H'). (I-M) At P7, there appears to be a similar overall number of CD45+ cells (I,J) and AIF1+/MHCII+ macrophages (K,L) in controls versus cKO testes. However, there are macrophages within the tubule lumen (dashed outlines in K' and L') only in cKO testes (arrows in L'), which engulf both Sertoli cells (black arrowhead in M) and TRA98+ germ cells (white arrowheads in M). Thin scale bar, 100 μm; thick scale bar 25 μm. (N) Graph showing average percent of tubules containing immune cells in control versus cKO tubules at E18.5, P7, P24, and P90 (E18.5: n=40 tubules each from 3 independent males; P7: n=40 tubules each from 3 independent males; P24: n=40, 36, 39 tubules each from 3 independent males; P90: n=27, 36, 37 tubules each from 3 independent males). Data are shown as mean ± SD. *P* values were calculated using a two-tailed Student t-test.

Figure S7

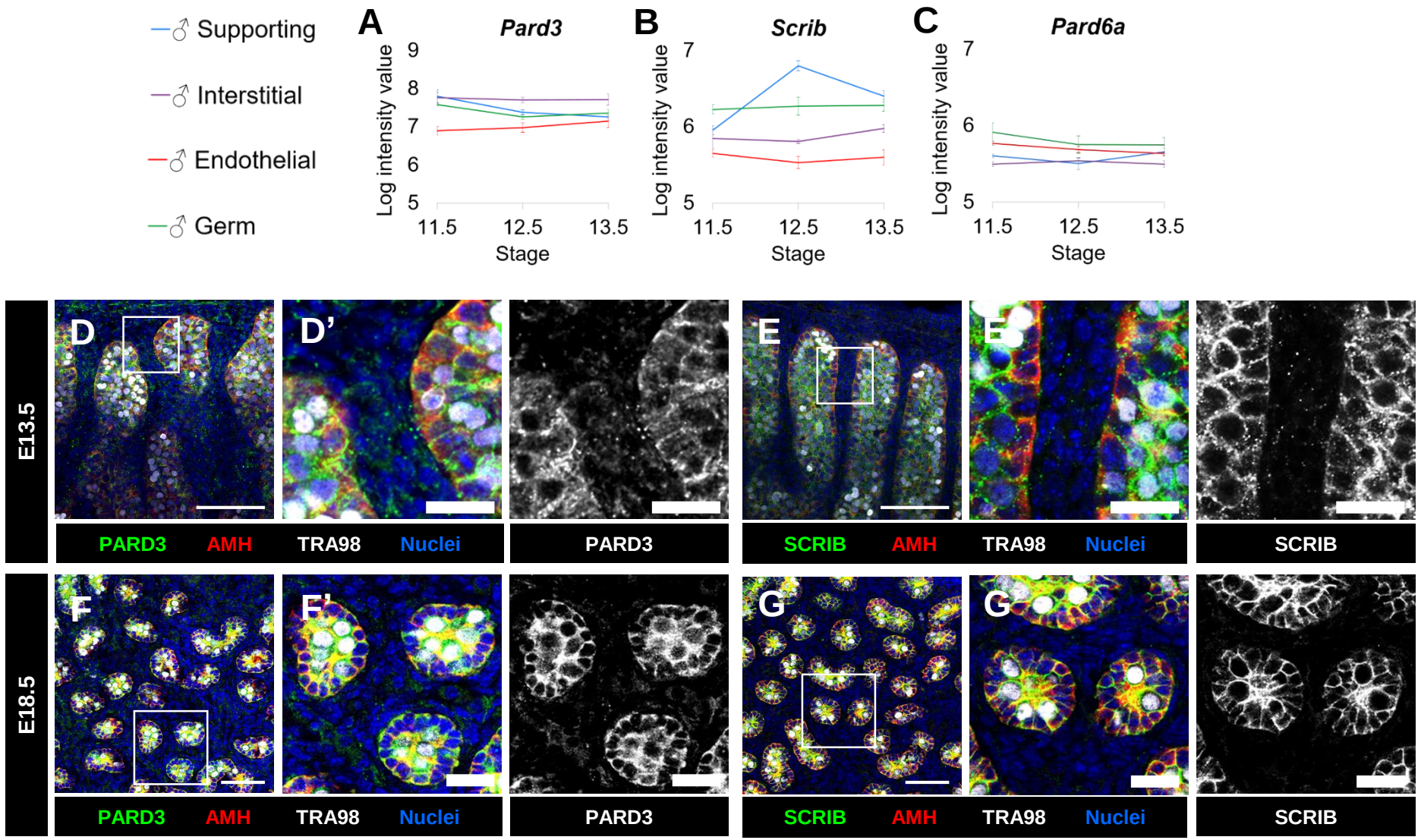
Supporting
Interstitial
Endothelial
Germ
A
Pard3
B
Scrib
C
Pard6a
Log intensity value
Stage
11.5
12.5
13.5
E13.5
E18.5
D
D'
E
E'
F
F'
G
G'
PARD3
AMH
TRA98
Nuclei
SCRIB

Figure S7. Apicobasal polarity markers are not specifically localized in fetal Sertoli cells, Related to Figure 7.

(A-C) Plots showing expression levels of apicobasal cell polarity genes *Pard3* (*Par3*), *Scrib* (*Scribble*), and *Par6da* (*Par6*), which were generated from fetal gonad cell-type-specific microarray data (Jameson et al., 2012), where cell lineages (supporting Sertoli cells, interstitial cells, endothelial cells, and germ cells) were independently plotted in different colors. Graph contains data for E11.5, E12.5, and E13.5 XY gonads for each cell type. In general, expression values below 6 are considered background expression levels. Overall, cell polarity genes in the fetal testis are either expressed non-specifically, i.e., in additional cell types other than Sertoli cells, and/or at very low/background levels. (D-G) Immunofluorescence images of E13.5 CD-1 (D,E) and E18.5 *Dhh*-Cre; $Rac1^{flox/+}$ control (F,G) fetal testes. D'-G' are higher-magnification images of the boxed regions in D-G. Apicobasal polarity markers PARD3 (apical) and SCRIB (basal) are both expressed in Sertoli cells at E13.5 and E18.5, but do not exhibit any specific subcellular localization or apicobasal enrichment. Thin scale bar, 100 μm; thick scale bar 25 μm.

Gene name	Sequence (5' to 3')
Amh forward	CCACACCTCTCTCCACTGGTA
Amh reverse	GGCACAAAGGTTCAGGGGG
Ar forward	CAGGAGGTAATCTCCGAAGGC
Ar reverse	ACAGACACTGCTTTACACAACTC
Cdh5 forward	TCCTCTGCATCCTCACTATCACA
Cdh5 reverse	GTAAGTGACCAACTGCTCGTGAAT
Cyp11a1 forward	GGAGGAAGCCGACAACAATGA
Cyp11a1 reverse	TCCACCTCACACGGTTCTCAA
Cyp17a1 forward	CAGAGAAGTGCTCGTGAAGAAG
Cyp17a1 reverse	AGGAGCTACTACTATCCGCAAA
Ddx4 forward	TACTGTCAGACGCTCAACAGGA
Ddx4 reverse	ATTCAACGTGTGCTTGCCCT
Dhh forward	GGCGCAGACCGCCTGATG
Dhh reverse	AAGGCACGGCCTTCGTAGTGG
Fshr forward	GGGATCTGGATGTCATCACT
Fshr reverse	GGAGAACACATCTGCCTCTA
Gapdh forward	AGGTCGGTGTGAACGGATTTG
Gapdh reverse	TGTAGACCATGTAGTTGAGGTCA
Gata1 forward	TGGGGACCTCAGAACCCTTG
Gata1 reverse	GGCTGCATTTGGGGAAGTG
Gdnf forward	GACTTGGGTTTGGGCTATGA
Gdnf reverse	AACATGCCTGGCCTACTTTG
Gfra1 forward (P7 assays)	CACTCCTGGATTTGCTGATGT
Gfra1 reverse (P7 assays)	AGTGTGCGGTACTTGGTGC
Gfra1 forward (P90 assays)	CCAATGTATCGGGCAGTACACA
Gfra1 reverse (P90 assays)	CCAGCGAGACCATCCTTTCC
Id4 forward	CAGTGCGATATGAACGACTGC
Id4 reverse	GACTTTCTTGTTGGGCGGGAT
Inhbb forward	GAGCGCGTCTCCGAGATCATCA
Inhbb reverse	CGTACCTTCCTCCTGCTGCCCTT
Kit forward	CATGGCGTTCCTCGCCT
Kit reverse	GCCCGAAATCGCAAATCTTT
Pdgfa forward	GACGGTCATTTACGAGATACCTC
Pdgfa reverse	CTACGCCTTCCTGTCTCCTC
Pou5f1 forward	GGAGGAAGCCGACAACAATGA
Pou5f1 reverse	TCCACCTCACACGGTTCTCAA
Sox9 forward	GCGGAGCTCAGCAAGACTCTG
Sox9 reverse	ATCGGGGTGGTCTTTCTTGTG
Srd5a1 forward	GAGTTGGATGAGTTGCGCCTA
Srd5a1 reverse	GGACCACTGCGAGGAGTAG
Stra8 forward	GCAGGTTGAAGGATGCTTTGAGC
Stra8 reverse	CCTAAGGAAGGCAGTTTACTCCCAGTC

Table S1. qPCR primers used in this study, Related to STAR Methods. Sequences of primers used for quantitative real-time PCR (qPCR) in this study (in alphabetical order).